Spinodal decomposition in a polymer solution

Nobuhiro Kuwahara and Kenji Kubota
Department of Biological and Chemical Engineering, Faculty of Technology, Gunma University, Kiryu, Gunma 376, Japan
(Received 3 December 1991)

The spinodal decomposition in a critical mixture of polydimethylsiloxane–diethyl carbonate was investigated by a time-resolved light-scattering technique, focusing especially on the early and the intermediate stages of phase separation. The most essential characteristics of this system are that both the refractive index and the density of the solvent and of the polymer are almost the same, and the effects of multiple scattering and sedimentation are mostly eliminated. The exponential growth of the scattered light intensity without changing of its wave number was clearly observed, in good agreement with Cahn-Hillard theory. The second peak, adding to the main (most dominant) peak, was found in the higher-scattering-angle region in the spectrum, characteristic of the intermediate stage. The scaled time dependences of the wave numbers of both peaks are well represented, respectively, by a master curve for various quenching depths by use of the characteristic wave number and time determined from the time dependence of the scattered light intensity at the early stage of spinodal decomposition. The quench depth dependence of the interdiffusion coefficient and of the wave number, where the most dominant fluctuation grows first in the unstable region, are in good agreement with three-dimensional Ising-model values, indicating the validity of the symmetric law of critical-point universality.

PACS number(s): 64.70.−p, 64.90.+b, 78.20.Dj

INTRODUCTION

If a mixture is brought from the one-phase region to the two-phase region by changing the thermodynamic state variables, then the temporal concentration fluctuation becomes unstable, and phase separation occurs. Phase separation in the unstable and unmixing mixture may proceed either by nucleation growth or by spinodal decomposition [1]. The dynamics in this unstable region especially in critical mixtures has been of great interest and has been investigated by many groups [2]. Recently, the analysis of the demixing kinetics becomes an important subject from the point of view of controlling and designing the structure and the functions of polymer blend systems [3]. On the other hand, the process of spinodal decomposition is a nonequilibrium phenomenon and is an attractive object for understanding the correlation and the cooperativity of various fluctuation modes. Cahn and Hillard presented the pioneering study to characterize the process of spinodal decomposition using the linearized theory [4,5]. Later, Cook extended this theory by introducing the effect of thermal fluctuations in the system [6].

There have been numerous theoretical [7–16] and experimental [17–33] works and significant advances have been achieved since the work of Cahn. Experimental investigations of simple liquid mixtures [17–21,29,30], polymer solutions [22,23,33], polymer-polymer mixtures [24–28,21,32], as well as metallic alloys [34–36] and glass forming mixtures [37] were analyzed by the concept of spinodal decomposition. It has been observed that the time evolution of phase separation can be divided essentially into three stages, namely, early, intermediate, and late stages, characterizing the behavior of phase separation and the scattering profiles [26]. As for the polymer-polymer mixtures, deGennes [38] and Pincus [39] presented the theoretical framework by adapting the Cahn-Hillard theory on the basis of Flory-Huggins-type description for free energy [40] (mean-field treatment), and from this viewpoint various polymer-polymer mixtures have been analyzed successfully so far [2]. For example, Hashimoto *et al.* studied polymer blend systems and found that the time evolution of the wave number of most dominant fluctuation (highest peak intensity) is well scaled by the characteristic wave number and time obtained from the behavior in the early stage and the one master curve is obtained. Moreover, the shape of the structure function is agreeable qualitatively with recent Furukawa theory [15,27]. However, the behavior in the neighborhood of the critical point in the stable one-phase region has not been well analyzed though it is quite necessary for characterizing the process of spinodal decomposition [41]. On the other hand, in the case of simple liquids and polymer solutions, where the mean-field theory is not valid but the three-dimensional Ising model is valid, the behavior in the neighborhood of the critical point is well characterized [42,43]. There have been several difficulties in the detailed analyses because the phase separation proceeds fairly quickly and the early stage, which is the time region covered principally by the Cahn-Hillard theory, has not been well observed so far [17–21,29,30]. Therefore, the analyses of the kinetics (time evolution) of spinodal decomposition have been rather restricted in the coarsening processes and/or the later stage of spinodal decomposition which follows the early stage of the initial linear growth regime predicted by Cahn [4,5]. Although many useful advances have been obtained from these works, sufficient understanding of the early and intermediate stages has not yet been attained. Moreover, from the viewpoint of experiment,

there are several essential problems such as multiple scattering and the sedimentation effect. All theories treat single scattering. Since multiple scattering distorts the scattering profiles, it made difficult detailed comparison between the experiment and the theory [44]. The sedimentation effect, which causes a concentration gradient, results in the distortion of the concentration distribution in the sample. It should be noted that Beysens, Guenoun, and Perrot performed an interesting experiment under microgravity using the sounding rockets [30]. They studied the late-stage behavior by direct visualization using a camera and a CCD camera, and reported the power-law behavior of the scaled time evolution that the characteristic length scale is expressed in proportion to time in combination with the results of light-scattering measurements of the density matched sample by deuteration [29].

In this paper, we will present experimental studies of spinodal decomposition of a polymer solution where multiple scattering and sedimentation effects are sufficiently eliminated, focusing especially on the early and intermediate stages. The early stage is clearly observed because of the long characteristic time due to high viscosity resulting from the polymer effect with the aid of a high speed and a high-resolution detecting system developed recently in our laboratory [45,46].

EXPERIMENT

Apparatus

The experimental setup used in the present study is shown in Fig. 1. The sample cell of fused quartz with 2-mm thickness and 10×20 mm^2 of width and height is placed in a temperature-regulated silicon oil bath. The cell is connected to the pressure line to apply the pressure into the sample cell by use of mercury. The applied pressure is read with the accuracy of 0.2-mm Hg by the mercury manometer. The sample solution contacts not only with the quartz glass of the cell but with the mercury; this makes thermal conductance and temperature distribution better. The temperature of the silicon oil bath is regulated within ±0.2 mK over 2 h, and the temperature

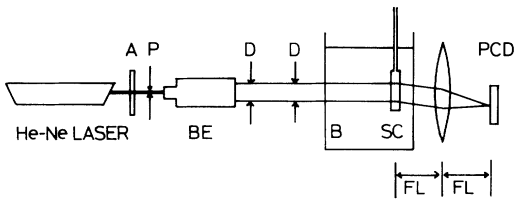

FIG. 1. Experimental arrangement for the measurements of spinodal decomposition. *A*, *P*, BE, *D*, *B*, and SC denote the neutral density filter attenuating the incident beam of the He-Ne laser, pinhole, beam expander, diaphragm, silicon oil bath, and sample cell, respectively. PCD is the photodiode array. FL denotes the focal length of the lens. The optical rays are shown to help the reader understand the role of the (Fourier-transform) lens. The sample cell is connected to the pressure line for quenching into the unstable region by the pressure jump method.

is monitored by a quartz thermometer which is placed very close to the sample cell. The incident He-Ne laser beam, with a wavelength of 632.8 nm in vacuum, was attenuated up to less than 0.1 mW by a neutral density filter to avoid unnecessary heating effect by a laser beam. The beam is expanded by the laser beam expander, passes through the diaphragms, and then illuminates the wide area of the sample. The scattered light is collected by the lens (diameter = 12 cm and focal length = 15 cm), which is placed at the focal length position from both the sample and the detector. The lens works as a Fourier-transform lens, and a (two-dimensional) Fourier-transformed image of the sample is obtained at the detecting plane. The detail is described elsewhere [46]. By the setup mentioned above the scattered light is integrated and averaged over the wide scattering area of the sample by use of a Fourier-transform lens. Our optical system greatly reduces the granular pattern (speckles) due to the high coherency of the incident laser beam, and a highly smooth scattering profile with high signal-to-noise ratio is obtained. This system is especially useful for the case of relatively low-scattering-angle measurements, such as the present experiment. The amount of the angular resolution is estimated to be less than 0.1°. The detector is a one-dimensional photodiode array (PCD, S2301-512Q, Hamamatsu Photonics, 512 channels with 50-μm width of each channel) and the scattered light intensity is obtained as a photocurrent signal of photodiode with very high speed. Ten scans are averaged for each elapsed time. The photocurrent signal is I/V converted, digitized by 16-bit high-speed analog-to-digital convertor, and then transported to a computer. The intensity of the unscattered transmitted light detected by the same PCD is used for the turbidity measurement and correction of attenuation for the scattered light intensity. The position of the transmitted light on PCD is used for the calculation of the scattering angle for each channel of PCD.

Sample preparation

In the present work a critical mixture of polydimethylsiloxane (PDMS) and diethyl carbonate (DEC) was used [43]. PDMS was fractionated first into three fractions from the original sample and then the middle fraction was further fractionated into 18 fractions by the fractional solution technique, using ethyl formate as a solvent. That is, the middle fraction of PDMS–ethyl-formate solution at a concentration less than 0.01 wt % was kept at a temperature a little below its phase-separation temperature in a thermostated water bath whose temperature was controlled to within ±1 mK. After the phase equilibrium was attained the dilute solution phase was separated from the other concentrated phases. Thus, the lower molecular weight PDMS sample with narrower molecular weight distribution was obtained. The concentrated phase was diluted successively by reagent grade ethyl formate for further fractionations. In this work, the fraction characterized as $M_w=8.0\times10^4$ and $M_w/M_n<1.02$ was used as a sample, M_w and M_n being the weight-averaged and the number-averaged molecular weight, respectively. Reagent grade DEC was thorough-

ly dried over anhydrous potassium carbonate and was fractionally distilled using a column of 140-cm length and 15-mm diameter packed with Rasching glass rings. Preparation of the solutions was achieved in a dry box under dried nitrogen gas in order to avoid the mixing of moisture.

The critical mixing point [$T_c = 34.42\,^{\circ}\mathrm{C}$, $w_c = 12.1_0$ wt %] was determined from the coexistence curve whose details were described elsewhere [43]. The reproducibility of T_c over the short and long periods was also described previously [22]. The critical point was ascertained by a precise coincidence with the precipitation threshold point. The solution of the critical concentration was put into the quartz cell by substitution of mercury not to make the gas phase.

The most essential feature of the PDMS-DEC system is that the multiple scattering and the density difference between PDMS and DEC are reduced very much. The difference of the refractive index between PDMS and DEC is ~ 0.021 at 25 °C and the difference of the density is ~ 0.0005 g/cm^3 at 25 °C. In taking account of the asymptotically symmetric shape of the coexistence curve [42], the effective density difference between two phase-separating phases is much less (say, less than one-tenth of the above value). Therefore, the progress of macroscopic phase separation into two coexisting phases should be greatly slowed down. It significantly reduces the problem of the stability of the sample (sedimentation due to density difference) arising from such a macroscopic phase separation in the time course of the progress of spinodal decomposition.

Procedure

The quench of the sample from the stable one-phase region to the unstable two-phase region was carried out by the pressure jump method to attain a quick and accurate response and to avoid unnecessary turbulence to the sample solution by the temperature jump method [18]. The critical point in a binary mixture is a point on the critical line according to the thermodynamic phase rule. The value of dT_c/dp is determined to be 8.8_5 mK/atm in the present system. Since only a slight elevation of pressure is necessary to get the quench of a few millidegrees Kelvin, the pressure jump method is quite effective. In other words, an elevation of the pressure causes the shift of the phase diagram. After ascertaining the critical temperature at the atmospheric pressure the pressure of the sample solution is elevated, and then the temperature of the bath is lowered to the final temperature of a desired quench depth. After complete equilibrium is achieved, the pressure is lowered to the atmospheric pressure. Thus, the quench into the unstable region is carried out. The pressure jump is essentially an adiabatic process and the adiabatic pressure decrease causes the temperature decrease of the system. This adiabatic temperature change decays sufficiently within at most 10 s after the pressure change, according to the simple estimation of thermodynamic quantities of the sample solution. Because heat exchange is accelerated by mercury separator for the application of pressure and the heat of mixing is liberated accompanying the demixing, the time for attaining the equilibrium at the final temperature should be less than the above estimate. The critical temperature (T_c) was measured every time before each experiment to determine the precise quench depth. After each experiment, the temperature of the phase-separated solution was increased and the sample solution was thoroughly stirred using a small teflon-coated magnet for the next measurements.

DATA ANALYSIS

The Cahn-Hillard theory is based on the linearization of a generalized diffusion equation and should be valid in the early stage of spinodal decomposition [4,5]. Considering the thermal noise effect introduced by Cook as a modification to the Cahn theory [6], the time evolution of the structure factor in the time course of spinodal decomposition is expressed by the following equation:

$$S(q,t) = S_x(q) + [S(q,0) - S_x(q)]\exp(2R_q t)\,, \tag{1}$$

where $S(q,t)$ is the overall structure factor and $S_x(q)$ is the virtual structure factor arising from the thermal noise. The quantity q is the wave number [the magnitude of the scattering wave vector $(4\pi n/\lambda)\sin(\theta/2)$, where n, λ, and θ are the refractive index of the sample, the wavelength of the incident beam in vacuum, and the scattering angle, respectively], t is time after the quench into the unstable region, and R_q is the growth rate characterizing the time evolution of spinodal decomposition. The measured scattered light intensity $I(q,t)$ is proportional to $S(q,t)$. Owing to the contribution of the $S_x(q)$ term to $S(q,t)$, the use of the simple semilogarithmic plot of $S(q,t)$ or $I(q,t)$ against t which has been frequently used would fail to obtain the precise determination of R_q [31]. Sato and Han presented a clever method to estimate R_q from $I(q,t)$ described by the 1/3-power plot as [31]

$$\{t/[S(q,t) - S(q,0)]\}^{1/3} = \{2[S(q,0) - S_x(q)]R_q\}^{-1/3} \times [1 - \tfrac{1}{3}R_q t + \tfrac{1}{81}(R_q t)^3 + \cdots]. \tag{2}$$

As the second-order term in t is absent in Eq. (2), this equation can be well approximated by a linear equation in t at $R_q t < 1$. The growth rate R_q is given as

$$R_q = -Mq^2(\chi^{-1} + 2Kq^2)\,, \tag{3}$$

where M is the diffusion mobility and χ is the composition susceptibility defined as $\chi^{-1} = (\partial^2 f/\partial\phi^2)_\theta$ with f and ϕ being the Helmholtz free energy and composition, respectively. The susceptibility χ is negative and K is the constant related to the contribution of interfacial free energy. The interdiffusion coefficient D^* which characterizes the kinetics of the spinodal decomposition is related to R_q by

$$D^* = -M/\chi \tag{4}$$

so that

$$R_q = D^* q^2 - 2MKq^4 = D^* q^2(1 - q^2/2q_m^2)\,, \tag{5}$$

where q_m $[=\frac{1}{2}(D^*/MK)^{1/2}=(\frac{1}{2})(-\chi K)^{-1/2}]$ is the wave number where the growth rate has a maximum value in the early stage and should be the same as the value of $q_m(t)$ at $t=0$, where $q_m(t)$ is the wave number corresponding to the peak intensity of $S(q,t)$. The value of $q_m(0)$ thus obtained should coincide with the wave number at the maximum position of scattered light intensity. In the linearized theory which accounts for the behavior in the early stage, the most dominant fluctuation with the wave number of $q_m(0)$ grows without the change of magnitude of its wave number.

With the evolution of the composition fluctuation the linear approximation of the Cahn-Hillard theory becomes invalid. The wave number of the most dominant fluctuation changes and decreases with time. The scattered light intensity also increases with time. These are the signals of the onset of the intermediate stage. The scaling relations have been studied in order to characterize the behaviors of $q_m(t)$ and $I_m(t)$ with time, $I_m(t)$ being the maximum scattered light intensity of the angular distribution of the scattering profile, as [8,47]

$$q_m(t)\sim t^{-a} , \tag{6}$$

$$I_m(t)\sim t^{b} . \tag{7}$$

The scaling idea has been further developed and introduced that one characteristic wave number q_c (or the characteristic length scale L_c) appears to be relevant in the evolution of the phase separation in spinodal decomposition. Any physical quantities should depend on time through the characteristic length scale in the scaling idea [15]. The characteristic time t_c is also related with such a length scale through the interdiffusion coefficient as

$$q_c=q_m(0) , \tag{8}$$

$$L_c=1/q_c , \tag{9}$$

$$t_c=1/(D^*q_c^2) . \tag{10}$$

These equations mean that the length and time scale governing over the whole time region should be determined by the behavior in the early stage. For the estimation of L_c and D^*, the values of correlation length and diffusion coefficient in the one-phase region in the neighborhood of the critical point have been used in some cases [17–21]. Use of the quantities in the one-phase region is still an open question to be clarified later on. The exponents related to the reduced temperature $(\epsilon=|T-T_c|/T_c)$ in the one-phase region have been well established for the three-dimensional Ising model systems. Using the characteristic wave number and time, $q_m(t)$ should be rescaled in reduced units as

$$Q_m(\tau)\sim\tau^{-a} , \tag{11}$$

where $Q_m(\tau)=q_m(t)/q_m(0)$ and $\tau=t/t_c$, respectively. There are various theoretical arguments about the magnitude of a in the intermediate and late stages. However, it is considered that the τ dependence of $Q_m(\tau)$ should be expressed by the system-independent universal equation. The time region after the early stage is divided by the behavior of $Q_m(\tau)$ with the elapsed time as the intermediate and late stages. The schematic representation of the behavior of the dominant fluctuation in spinodal decomposition discussed in the paper by Hashimoto is very suggestive [25,26].

For the scaling approach concerning the time evolution of spinodal decomposition, Furukawa proposed a simple form for the universal curve for the critical fluid mixtures shown as [15]

$$Q_m(\tau)^{-1}-1-((A/B)^{1/2}\{\tan^{-1}[Q_m(\tau)^{-1}(B/A)^{1/2}] -\tan^{-1}[(B/A)^{1/2}]\})=B\tau , \tag{12}$$

where A and B are the adjustable parameters.

The dominant fluctuation of the composition reaches the final compositions of separated two-phase regions in equilibrium with the further progress of time. There exists the self-similarity between the structure developed at different times, and the structure factor has some characteristic shape. Furukawa proposed an idea of the dynamical scaling for the structure function in the late stage taking account of the domain connectivity corresponding to the most dominant fluctuations as [15]

$$S(q,t)\sim[L(t)]^3F(qL(t)) , \tag{13}$$

where $L(t)$ is the single length parameter in the late stage and $F(x)$ is the universal scaling function for the critical mixture defined by

$$F(x)=4x^2/(3+x^8) . \tag{14}$$

Then, the q^{-6} tail in the structure function suggests the self-similar evolution of the fluctuation. Moreover, with the appearance of a well-developed domain wall (interface) the q^{-4} tail (Porod's law) [48] appears and it reflects the local structure in the overall phase-separating structure compared with the q^{-6} tail.

RESULTS AND DISCUSSION

In Fig. 2 we present the typical sets of the results of low angle scattering measurements for 3.5- and 6.5-mK quenches (sample codes C and E, respectively) at various elapsed times after the quench into the spinodal region. The region of the central transmitted light is not shown and only every fourth point is shown to avoid cluttering. Similar results are obtained for other quenches. The peak in the scattering profile corresponds to the spinodal ring. Even at the last scan of measurements in Fig. 2, the transmitted light decays only about 5% from the initial value. The turbidity does not increase as much in the time course of phase separation. The multiple-scattering effect should be small enough, and it makes the data analysis in the time course of spinodal decomposition quite simple. A little density difference in PDMS and DEC ensures the stability and homogeneity of the sample. Therefore, in the experimental time range we are able to analyze without any correction due to macroscopic phase separation because of the use of a wide range of scattering volumes and a Fourier-transform lens. Since one of the components (PDMS) is a macromolecular substance and the viscosity of the sample solution is fairly high, enough to slow down the progress of phase separa-

tion in the spinodal region, it makes the observation of the time dependence of the scattering function easy. The most characteristic points in Fig. 2 are as follows. (1) The early stage of the spinodal decomposition is clearly observed in the experimental q range. (2) The second peak adding to the main peak, which is normally observed and analyzed in the time evolution of spinodal decomposition, appears at the higher-scattering-angle region though the intensity is less than that of the main peak and is not observed in the early stage [32]. (3) After the early stage, both peaks grow in intensity and decrease in scattering angle with time. (4) The second peak appears as a definite peak at first and seems to form a shoulder of the main peak. This feature seems to be more accelerated for deeper quench, where the first appearance of the main peak shifts to a higher wave number. (5) The peak position of both peaks is smaller in q for the shallower quench. (6) The position of the second peak is about five times as large as that of the main peak. This may be the reason why the second peak has not been observed before.

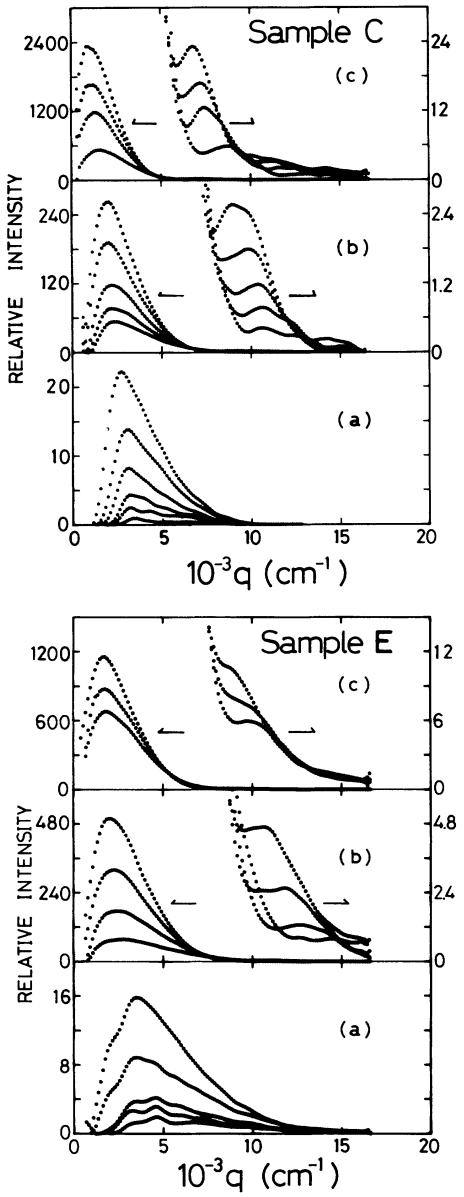

FIG. 2. Time evolution of the angular profiles of scattered light. Sample C (a) is for the quench depth (ΔT)=3.5 mK and sample E (b) is for ΔT=6.5 mK. The elapsed time after the start of phase separation for sample C is (a) 30, 100, 170, 270, 370, and 470 s, (b) 770, 970, 1170, 1370, and 1550 s; (c) 1920, 2670, 3420, and 4170 s from the bottom to the top, respectively. The elapsed time for sample E is (a) 50, 80, 110, 150, and 210 s; (b) 450, 650, 850, and 1050 s; (c) 1250, 1450, and 1750 s from the bottom to the top, respectively. For sample E the second peak becomes a shoulder at the last time. The arrow indicates the scale of (relative) intensity for the main (dominant) peak and the second peak.

In order to obtain the parameters characterizing the early-stage spinodal decomposition, we may use the linearized theory of Cahn described in the section of data analysis. The method by Sato and Han is used to determine R_q, and then D^* and $q_m(0)$ were determined from the plot of R_q/q^2 versus q^2, respectively. A 1/3-power plot for the 3.5-mK quench is shown in Fig. 3. The same analysis was carried out for the 6.5-mK quench. Only the data for eight scattering angles are shown as representative results. The results for other scattering angles show a similar tendency as shown in Fig. 3. The data points are shifted to avoid cluttering as noted in the caption. For two curves of lower scattering angles, the first several points are omitted because the scattered intensity is so low and its uncertainty is fairly large. Good linearity is obtained in an early time since $R_q t < 1$ for $t < 600$ s and a 1/3-power plot is valid. The deviation

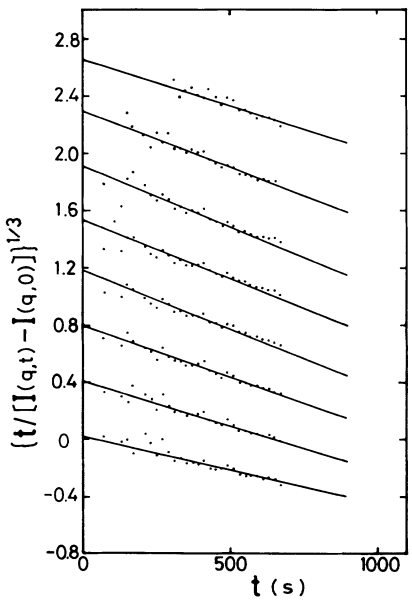

FIG. 3. The 1/3-power plot for sample C (ΔT=3.5 mK). t denotes the elasped time. Each data set except for the third curve from the top is shifted vertically. The wave vector and the amount of shift for each data set from the top to the bottom are, respectively, 2650 cm^{-1}, 0.8; 2980 cm^{-1}, 0.4; 3310 cm^{-1}, 0; 3640 cm^{-1}, −0.4; 3970 cm^{-1}, −0.8; 4300 cm^{-1}, −1.2; 4630 cm^{-1}, −1.6; and 4970 cm^{-1}, −2.0. Good linearity is observed.

from the straight line is observed over ~600 s, and reflects nonlinear phenomena of the phase-separating process and indicates the onset of the intermediate stage of spinodal decomposition. R_q determined from the slope in Fig. 3 is shown in Fig. 4(a) as a function of q^2. The maximum in R_q suggests the existence of the early stage of spinodal decomposition in the present system. Until now, any clear observation of the appearance of the early stage, especially for binary liquid mixtures, has not been presented. As far as we know, this observation is the first direct one of the early stage of spinodal decomposition for such a system. The wave number at the maximum of R_q corresponds to $q_m(0)$ in Eq. (5). This $q_m(0)$ value agrees well with the peak position of the scattering function in Fig. 2. The plot of R_q/q^2 versus q^2 is shown in Fig. 4(b). For $q^2 > 2[q_m(0)]^2$, the plot of R_q/q^2 shows the tendency to deviate from the straight line due to the effect of thermal noise. The quantities of D^* and $q_m(0)$ were obtained from the intercept and the slope of the linear portion of the plot. The $q_m(0)$ value determined from the intercept of the q^2 axis also agrees well with the wave number of the peak of the scattering function for the beginning of spinodal decomposition. In the analysis of $q_m(t)$ versus time, $q_m(t)$ indeed does not change its magnitude for small $\tau(\tau<1)$ as discussed below. It is worthwhile to note that Bates and Wiltzius analyzed their results for polybutadiene isotopic mixture and obtained good linearity in R_q/q^2 versus q^2 [32]. However, they could not observe the scattering peak to remain stationary at the earliest measurable time. Higgins, Fruitwala, and Tomlins measured the spinodal decomposition of a polymer blend of poly-(α-methyl-styrene-coacrylonitrile) and poly(methyl methacrylate) using small-angle neutron scattering [49] and observed the discrepancies between the peak wave number corresponding to the maximum R_q in the plot of R_q versus q and $q_m(0)$, determined from the q^2-axis intercept of the plot of R_q/q^2 versus q^2 and/or the initial peak position of the scattering function. They used the semilogarithmic plot of $I(q,t)$ against time to determine R_q. As is discussed by Sato and Han, the semilogarithmic plot could include an error in the determination of R_q due to the contribution from the virtual structure factor arising from the non-negligible thermal noise. The inconsistency of the use of Eq. (5) in the analysis of Higgins, Fruitwala, and Tomlins may have resulted from the thermal noise effect. The consistency of $q_m(0)$ determined from (1) the peak of R_q, (2) the intercept of the q^2-axis in the plot of R_q/q^2, and (3) the peak position of the scattering function just after the quench suggests that Cahn's linearized theory is valid in the early stage of spinodal decomposition and a 1/3-power plot is also suitable for the determination of R_q in our case. The parameters characterizing the early stage of spinodal decomposition are tabulated in Table I.

The scaled time evolution of the scaled wave number of the peak position of the main and second peaks is shown in Fig. 5 for the quench depths of 3.5 and 6.5 mK. The lower curve denotes the relationship for the main (dominant) peak and the upper curve denotes that for the second peak. One master curve is obtained for both peaks and it is ascertained that the scaling does hold over the time range of $0<\tau<20$ using scaling parameters determined in the early stage. It should be noted that not only the main peak but the second peak are well scaled and $Q_m(\tau)$ remains unchanged with time in the time range of $\tau<1$. The relationship of $Q_m(\tau)$ with τ for several quench depths in the present work is shown in Fig. 6 in the double-logarithmic plot. It is also noted that the scaled relation of $Q_m(\tau)$ with τ holds well for both the main and second peaks and the universal master curve is obtained. The second peak forms a shoulder of the main peak with the increase of time for deeper

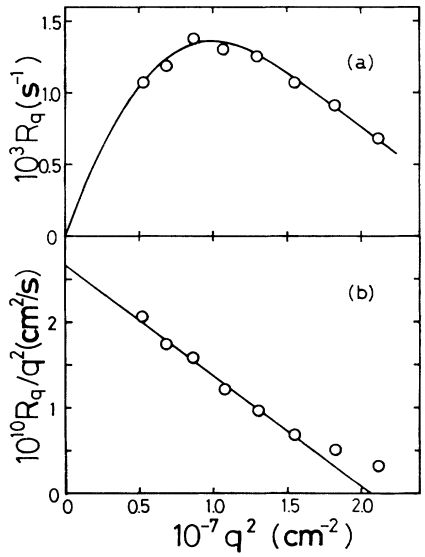

FIG. 4. The growth rate R_q (a) and R_q/q^2 (b) as a function of the squared wave number q^2 for sample C. The values of R_q are determined from the slope of the 1/3-power plot in Fig. 3. The interdiffusion coefficient D^* is determined by the intercept of R_q/q^2 as is shown by the straight line in (b). Linearity is good. The wave number which gives the maximum of R_q is in good accordance with half of the value which gives $R_q/q^2=0$ by this straight line.

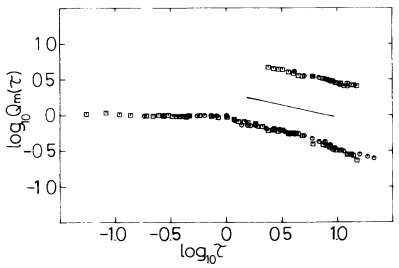

FIG. 5. The scaled time evolution of the scaled wave number of the peak positions of the main and second peaks for samples C and E. The scaling factors (characteristic time and wave number) are $1/D^* q_m(0)^2$ and $q_m(0)$, respectively, and are determined from the linearized theory for the early stage. The symbols □ and ○ denote the results for samples C and E, respectively. Superposition is very good and the universal master curve is obtained. It should be noted that none of the adjusting parameters are used in this plot. The slope of the insetted line is $-1/3$.

TABLE I. Parameters characterizing the early stage of spinodal decomposition.

Sample code	$\Delta T(=T_c-T)$ (mk)	$10^6\epsilon$[a]	$10^{-3}q_m(0)$ (cm^{-1})	10^4L_c[c] (cm)	$10^{10}D^*$ (cm^2/s)	t_c[d] (s)
A	2.1	6.8_3	2.28	4.39	2.09[b]	920
B	2.5	8.1_3	2.37	4.22	2.24[b]	794
C	3.5	$11._4$	3.21	3.12	2.66	364
D	4.8	$15._6$	3.74	2.67	3.75[b]	190
E	6.5	$21._1$	4.63	2.16	4.27	109
F	14.5	47.1	8.31[b]	1.20	5.76[b]	25.1

[a]Critical temperature (T_c) is 34.42 °C and $\epsilon=|T-T_c|/^\circ T_c$.
[b]These values are determined by superposing the curve of $q_m(t)$ vs t to the curve of $Q_m(\tau)$ vs τ obtained for samples *C* and *E*.
[c]$L_c=1/q_m(0)$.
[d]$t_c=1/D^*q_m(0)^2$.

quench depth. It is emphasized that the existence of the stationary region of $Q_m(\tau)$ in $\tau<1$ is clear.

The quench depth dependence of $q_m(0)$ and D^* is observed as is shown in Table I. From the viewpoint of the symmetric law of the critical-point universality [42], $Q_m(0)$ and D^* in the unstable spinodal region should obey the same power law as in the stable one-phase region and have the same exponents as the critical exponents against ΔT ($=|T-T_c|$). A detailed study of the critical behaviors in the one-phase region has been carried out for the present system and the ΔT dependence of the relevant values (correlation length and diffusion coefficient) is given by [22,50]

$$\xi_+=(7.13\pm1.71)\times10^{-8}\epsilon^{(-0.625\pm0.015)}\ (\text{cm})\ , \quad (15)$$

$$A=(3/8)\pi D_+\xi_+\ , \quad (16)$$

$$A=\lim(\Gamma/q^3)=7.02\times10^{-14}\ (\text{cm}^3/\text{s})\ , \quad (17)$$

where ξ_+ and Γ are the correlation length and the decay rate of the fluctuation in the one-phase region, respectively. The subscript + means that the value is defined in the one-phase region. The temperature dependences of $q_m(0)$ and D^* are shown in Fig. 7 in the double-logarithmic plot. The slope of $q_m(0)$ is evaluated to be 0.65 and the slope of D^* 0.62. These values are very close to 0.625 in the one-phase stable region by the relation of Eq. (9) and are consistent with the three-dimensional Ising model. Therefore, it is ascertained that the Ising model values for the exponents and the universal symmetric law are valid for the unstable region, too. Until now, the Ising model values are assumed in the analysis of the scaling relation in the time evolution of spinodal decomposition for low-molecular-weight binary mixture systems. Though a few direct determinations of

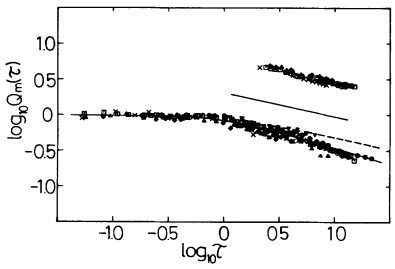

FIG. 6. The superposed scaled time evolution of the scaled wave number of the main and the second peaks. The superposition is carried out so that the curve of $q_m(t)$ versus t for each sample (*A*, *B*, *D*, and *F*) is superposed to the master curve obtained by Fig. 5. The notations of the symbols are, respectively, ◇, sample *A* ($\Delta T=2.1$ mK); Δ, sample *B* ($\Delta T=2.5$ mK); □, sample *C* ($\Delta T=3.5$ mK); ×, sample *D* ($\Delta T=4.8$ mK); ○, sample *E* ($\Delta T=6.5$ mK); and ∇, sample *F* ($\Delta T=14.5$ mK). Both peaks are well superposed with the same scaling factor. The slope of the insetted line is $-1/3$. The solid curve denotes the theoretical one calculated by the Furukawa theory (see text). The representative master curve for the simple binary liquid mixtures is also shown by the dashed curve [19,29,30].

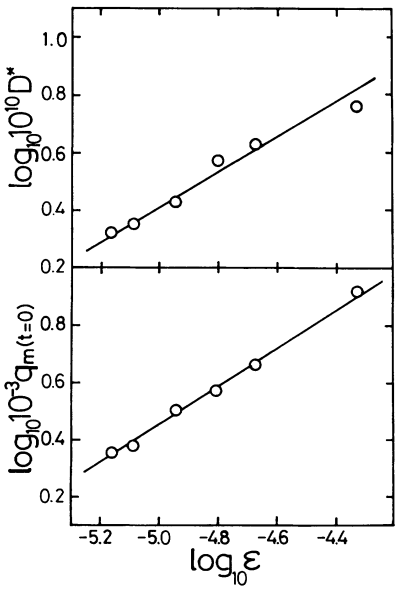

FIG. 7. The quench-depth dependence of the interdiffusion coefficient D^* and $q_m(0)$ plotted as the double-logarithmic plot. Both plots are well represented by the power-law relations. The exponents for D^* and $q_m(0)$ against the reduced temperature ϵ are 0.62 and 0.65, respectively, and are in good accordance with those in the stable one-phase region and the three-dimensional Ising model values.

$q_m(0)$ and D^* in the spinodal region are reported for the polymer-polymer mixtures and mean-field values are reported, the detailed study very near the critical point (the critical concentration and temperature) determined in the stable region is still left open and the symmetric law has not yet been ascertained. Although the agreement of the exponents is good, the agreement of the amplitude factors is not so good. The inverse of ξ_+ in the one-phase region which corresponds to $q_m(0)$ is about 3.6 times as large as $q_m(0)$ and the diffusion coefficient in the one-phase region is about 2.4 times as large as D^*. The reason for this discrepancy is not clear at the present time, but it is noteworthy that the ratio of the characteristic time of ξ_+^2/D_+ (in the stable region) to $1/D^*[q_m(0)]^2$ (in the unstable region) is about 0.031, $-\log_{10}(3.6)/\log_{10}(0.031)$ is $1/2.7 \sim 1/3$, and this discrepancy causes almost no apparent change in the plot of $Q_m(\tau)$ versus τ [22,23].

The deviation of $Q_m(\tau)$ from $Q_m(\tau)=1$ in the early stage in Fig. 6 indicates the onset of the nonlinear effect in the time evolution of component fluctuation and Cahn's linearized theory is no longer valid in the time region of $\tau > 1$. This time region is denoted as the intermediate stage of spinodal decomposition. The crossover from the early stage to the intermediate stage occurs around $\tau = 1$.

In the intermediate stage $q_m(t)$ or $Q_m(\tau)$ decreases with time. The tine dependence of $q_m(t)$ seems to be well expressed by the scaling relation of Eq. (6) with $a \sim 1/3$ [7,8] for both peaks; the exponent a is independent of time in the present system although the experimental time range is relatively restricted ($\tau < 20$). The Furukawa theory, as Eq. (12), has been studied for the time dependence of $Q_m(\tau)$. The solid curve in Fig. 6 is drawn using the values of $A=0.1$ and $B=0.14$ in Eq. (12). The value of $A=0.1$ is estimated so that the predicted behavior in the early stage recovers the prediction of Kawasaki and Ohta [11,15] and the value of $B=0.14$ is a little larger than the value of 0.045 used to fit the results of the low-molecular-weight binary mixture system (isobutyric acid and water and/or 2,6-lutidine and water). Beysens *et al.* have used $B=0.022$ [29] and 0.07 [30] for cyclohexane and methanol and Bates and Wiltzius [32] used $B=0.0195$ for polybutadiene isotopic mixture. Agreement between the experimental and theoretical master curves is good and the behavior of $Q_m(\tau)$ is well reproduced. The distinctive deviation from the $\sim 1/3$-power dependence of $Q_m(\tau)$ on τ is not observed yet at $\tau \sim 20$, as is seen in Fig. 6, and the intermediate stage seems to have a little long-time scale due to the small contribution of the interfacial tension. The interfacial tension plays an important role in the phase separation of the low-molecular-weight critical mixture systems, for example, isobutryic acid and water [19]. Siggia studied the long-time coarsening behavior based on the capillary flow model and finds the τ^{-1} dependence of $Q_m(\tau)$ [13]. Phase separation in the large-τ region is controlled by the interfacial tension too, and a crude estimate of such a region gives $(k_B T/\sigma)^{-1/2} > Q_m(\tau) > (\sigma/g\Delta\rho)^{-1/2}$, where k_B, σ, and $\Delta\rho$ are the Boltzmann constant, the interfacial tension, and the density difference of the two coexisting phases, respectively. The left-hand inequality gives the estimate of the onset of such a region. As the interfacial tension for the polymer solution has $M_w^{-1/2}$ dependence [51], its effect should be fairly low compared with the low-molecular-weight mixtures. In polymer solutions the time range of the intermediate stage may be enlarged by the small contribution of the interfacial tension similarly with the prolonged early stage by the polymer effect (increase of viscosity).

In Fig. 8 the reduced time dependence of the maximum scattered intensity $I_m(\tau)$ is plotted in the double-logarithmic plot. $I_m(\tau)$ increases gradually with time at first and the scaling relation of $I_m(\tau) \sim \tau^b$ holds in the range of $\tau > 1$ corresponding to the intermediate stage. In the intermediate stage, both the wavelength and the amplitude of the dominant fluctuation mode grow with time and the self-similar structure does not yet exist, and the scaling relation of $q_m(t)$ and $I_m(t)$ is not expressed by a single parameter. Therefore, the inequality $b > 3a$ should be applied [26]. The value of a is approximated to be about 1/3 as is shown in Fig. 6 and b is estimated to be about 2.2 as is shown in Fig. 8. The results of $I_m(\tau)$ against τ do not fall onto a universal curve and show substantial deviation with each other because of non-self-similarity in the intermediate stage.

The variation of the profile of the scattering function with the time of lapse as a function of the wave number with both being scaled by the peak intensity and peak wave number is shown in Fig. 9. Furukawa proposed a simple form for the structure factor in the region of a self-similar structure with the concept of dynamic scaling [15]. Equation (14) indicates that the tail of the structure factor is approximated by a q^{-6} dependence, which means the formation of a self-similar structure [25]. On the other hand, a q^{-4} dependence in the tail of the structure factor in the three-dimensional system is known as Porod's law and reflects the formation of the interface between two coexisting phases [48]. The q dependence of the scattering function is of great interest especially because there exists the second peak adding to the dominant main peak in our system. The top curve in Fig. 9 corresponds to $\tau = 2.6_6$ and to the beginning of the intermediate stage. The slopes around $\log_{10}(q/q_m) = 0.6$ and at the far right in the figure seem not to be expressed by any meaningful power-law relation as discussed above. The next two curves correspond to $\tau = 9.6_2$ and $\tau = 21_5$,

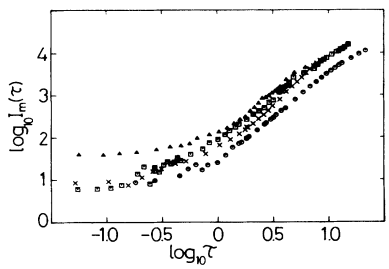

FIG. 8. The double-logarithmic plot of the peak intensity $\mathrm{Im}(\tau)$ of the main peak vs scaled time τ. The meanings of the symbols are the same as those in Fig. 6.

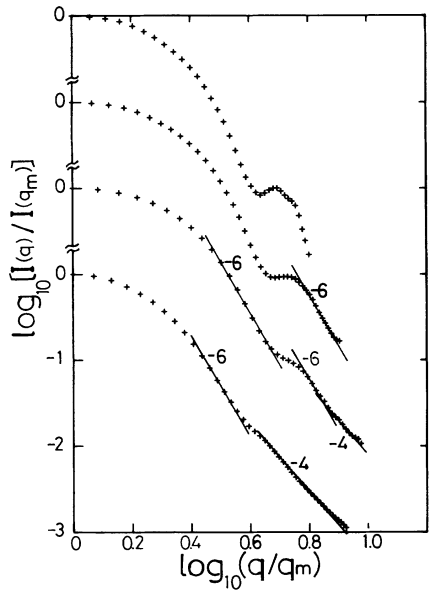

FIG. 9. The normalized structure factor as a function of the normalized wave number. Normalization is obtained by the intensity of the main peak $I(q_m)$ and the wave number of the main peak q_m, respectively. The scaled time for each curve is $\tau=2.6_6$ (sample C); $\tau=9.6_2$ (sample E); $\tau=21._5$ (sample E); and $\tau=180$ (sample F), from the top to the bottom, respectively. The numbers for respective insetted lines mean the value of the slope.

respectively. For the upper curve the slope around $\log_{10}(q/q_m)=0.6$ is not expressed by a q^{-6} dependence, but the slope at the far right is well expressed by a q^{-6} dependence. On the other hand, for the lower curve the slope around $\log_{10}(q/q_m)=0.6$ is now well expressed by a q^{-6} dependence, but the slope at the far right seems to be fitted by two lines of q^{-6} and q^{-4}. It seems that the region where the q^{-6} dependence holds decreases and the region where the q^{-4} dependence holds increases during this time region. The bottom curves shows the scattering profile at $\tau=180$ and may be in the late stage. The slope around $\log_{10}(q/q_m)=0.6$ is still well expressed by a q^{-6} dependence and the slope at the far right is well approximated by the line of a q^{-4} dependence. Takenaka, Hashimoto, and Jinnai analyzed their results for the late stage of spinodal decomposition and related such a q^{-4} dependence of the tail to the growth of local structure as the interface where semimacroscopic phase separation already occurs and the global structure has self-similarity [52]. In this context, the second peak reflecting the finer structure compared with the dominant peak should have a tendency to form self-similar structure a *priori* to the dominant mode and its time evolution may originate the formation of the interface between the final coexisting two phases at equilibrium. The appearance of a shoulder in the structure factor is recently predicted by several authors [16,32,52,53] though the position of such a shoulder is a little smaller in q/q_m ($q/q_m \sim 2-3$) than our present case ($q/q_m \sim 4-5$). Bates *et al.* and Takenaka *et al.* have found that the second peak appears only as a shoulder in contrast to our result. The scattered intensity of the second peak (or shoulder) is about two orders of magnitude less than that of the main peak, which is in accordance with theories [16,53]. The reason why the second peak in the PDMS-DEC system has a slightly higher wave number is not clear at present. This may be related with the asymmetry of components (polymer and low-molecular-weight solvent) and the broadness of the main peak, which is observed too in other polymer solutions, of polystyrene and cyclohexane by Lal and Bansil [33]. It should be noted that in our recent experiment of spinodal decomposition for isobutyric acid and water such a second peak is observed from the intermediate stage though it appears as a shoulder [54]. Therefore the origin of this second peak seems to be an important subject in the analysis of spinodal decomposition [55].

CONCLUSION

The time evolution of spinodal decomposition in a critical mixture of polydimethylsiloxane–diethyl carbonate was investigated by the time-resolved light-scattering method with the aid of a Fourier-transform lens for the sake of the improvement of the signal-to-noise ratio, expecially focusing on the early and intermediate stages of phase separation. The early stage of spinodal decomposition predicted by Cahn's theory was clearly observed and the linearized theory works very well. The second peak adding to the main (dominant) peak was found at the higher-scattering-angle region characteristic to the intermediate stage. The reduced wave numbers of both peaks are well scaled by the same reduced time resulting in the universal master curve using the characteristic wave number and interdiffusion coefficient determined in the early stage. These characteristic wave-number and interdiffusion coefficients are represented by a power-law dependence on the quench depth and the exponents show good agreement with the three-dimensional Ising model. The symmetric law of critical universality is ascertained for the critical exponents. The tail of the structure factor for the second peak has a tendency to have a q^{-6} dependence even in the intermediate stage and the shape of such a tail changes to result in a q^{-4} dependence finally in the late stage. This suggests that in the intermediate stage the most dominant component fluctuation mode does not reach final equilibrium concentration, but there exists another fluctuation mode (structure) having larger wave number and/or smaller wavelength, and a self-similar structure begins to be formed in the larger dominant fluctuation. Therefore, the mechanism of phase separation in spinodal region should not be understood only by the monotonous kinetics of the single fluctuation mode, and the understanding of the mechanism of the appearance of fine structure in the intermediate and late stages of spinodal decomposition should be quite important.

ACKNOWLEDGMENTS

The authors wish to thank Dr. Hamano of Gunma University for assemblage of a 512-channel photodiode array and for valuable discussions. They also wish to thank Mr. K. Takiwaki of Gunma University for his help in the measurements. This work was partly supported by the Grant-in-Aid from the Ministry of Education, Science and Culture in Japan.

[1] I. Prigogine and R. Defay, *Chemical Thermodynamics* (Longmans Green, London, 1954).
[2] For example, T. Hashimoto, Phase Transitions **12**, 47 (1988), and references therein.
[3] O. Olabisi, L. M. Robeson, and M. T. Shaw, *Polymer-Polymer Miscibility* (Academic, New York, 1979).
[4] J. W. Cahn, J. Chem. Phys. **42**, 93 (1965).
[5] J. W. Cahn and J. E. Hillard, J. Chem. Phys. **28**, 258 (1968).
[6] H. E. Cook, Acta Metall. **18**, 297 (1970).
[7] I. M. Lifshitz and V. V. Slyozov, J. Phys. Chem. Solids **19**, 35 (1961).
[8] K. Binder and D. Stauffer, Phys. Rev. Lett. **33**, 1006 (1974).
[9] J. S. Langer, M. Bar-on, and H. D. Miller, Phys. Rev. A **11**, 1417 (1975).
[10] K. Kawasaki, Prog. Theor. Phys. **57**, 826 (1977).
[11] K. Kawasaki and T. Ohta, Prog. Theor. Phys. **59**, 362 (1978).
[12] K. Binder, Phys. Rev. B **15**, 4425 (1977).
[13] E. D. Siggia, Phys. Rev. A **20**, 595 (1979).
[14] J. D. Gunton, M. San Miguel, and P. S. Sahni, in *Phase Transitions and Critical Phenomena,* edited by C. Domb and J. L. Lebowitz (Academic, New York, 1983), Vol. 8.
[15] H. Furukawa, Adv. Phys. **34**, 703 (1985).
[16] T. Koga and K. Kawasaki, Phys. Rev. A **44**, 817 (1991).
[17] W. I. Goldburg, C.-H. Shaw, J. S. Huang, and M. S. Pilant, J. Chem. Phys. **68**, 484 (1978).
[18] N.-C. Wong and C. M. Knobler, J. Chem. Phys. **69**, 725 (1978).
[19] Y. C. Chou and W. I. Goldburg, Phys. Rev. A **20**, 2105 (1979).
[20] Y. C. Chou and W. I. Goldburg, Phys. Rev. A **23**, 858 (1981).
[21] N.-C. Wong and C. M. Knobler, Phys. Rev. A **24**, 3205 (1981).
[22] N. Kuwahara, M. Tachikawa, K. Hamano, and Y. Kenmochi, Phys. Rev. A **25**, 3449 (1982).
[23] K. Hamano, M. Tachikawa, Y. Kenmochi, and N. Kuwahara, Phys. Lett. **90A**, 425 (1982).
[24] S. Nojima, K. Tsutsumi, and T. Nose, Polym. J. **14**, 225 (1982); S. Nojima, Y. Ohyama, M. Yamaguchi, and T. Nose, *ibid.* **14**, 907 (1982).
[25] T. Hashimoto, M. Itakura, and H. Hasegawa, J. Chem. Phys. **85**, 6118 (1986).
[26] T. Hashimoto, M. Itakura, and N. Shimidzu, J. Chem. Phys. **85**, 6773 (1986).
[27] M. Okada and C. C. Han, J. Chem. Phys. **85**, 5317 (1986).
[28] H. Meier and G. R. Strobl, Macromolecules **20**, 649 (1987).
[29] P. Guenoun, R. Gastaud, F. Perrot, and D. Beysens, Phys. Rev. A **36**, 4876 (1987).
[30] D. Beysens, P. Guenoun, and F. Perrot, Phys. Rev. A **38**, 4173 (1988).
[31] T. Sato and C. C. Han, J. Chem. Phys. **88**, 2057 (1988).
[32] F. S. Bates and P. Wiltzius, J. Chem. Phys. **91**, 3258 (1989).
[33] J. Lal and R. Bansil, Macromolecules **24**, 290 (1991).
[34] S. Katano and M. Iizumi, Phys. Rev. Lett. **52**, 835 (1984).
[35] M. Furusaka, Y. Ishikura, and M. Mera, Phys. Rev. Lett. **54**, 2611 (1985).
[36] S. Komura, K. Osamura, H. Fujii, and T. Takeda, Phys. Rev. B **31**, 1278 (1985).
[37] A. F. Craievich, J. M. Sanchez, and C. E. Williams, Phys. Rev. B **34**, 2762 (1986).
[38] P.-G. deGennes, J. Chem. Phys. **72**, 4756 (1980); P.-G. deGennes, *Scaling Concepts in Polymer Physics* (Cornell University, Ithaca, 1979).
[39] P. Pincus, J. Chem. Phys. **75**, 1996 (1981).
[40] P. J. Flory, *Principles of Polymer Chemistry* (Cornell University, Ithaca, 1953).
[41] K. Binder, Phys. Rev. A **29**, 341 (1984).
[42] H. E. Stanley, *Introduction to Phase Transitions and Critical Phenomena* (Oxford University, Oxford, 1971).
[43] M. Nakata, T. Dobashi, N. Kuwahara, M. Kanko and B. Chu, Phys. Rev. A **18**, 2683 (1978); N. Kuwahara, J. Kojima, and M. Kaneoko, *ibid.* **12**, 2602 (1975); K. Hamano, N. Kuwahara, and M. Kaneko, *ibid.* **20**, 1135 (1979).
[44] K. Hamano, N. Kuwahara, and M. Kaneko, Phys. Rev. A **21**, 1312 (1980).
[45] K. Kubota and N. Kuwahara, Phys. Rev. Lett. **68**, 197 (1992).
[46] K. Kubota and N. Kuwahara (unpublished).
[47] J. L. Lebowitz, J. Marro, and M. M. Kalos, Acta Metall. **30**, 297 (1982).
[48] G. Porod, in *Small Angle X-ray Scattering,* edited by O. Glatter and O. Krathky (Academic, London, 1982).
[49] J. S. Higgins, H. Fruitwala, and P. E. Tomlins, Macromolecules **22**, 3674 (1989).
[50] K. Kawasaki, Ann. Phys. (N.Y.) **61**, 1 (1970).
[51] J. F. Joanny and L. Leibler, J. Phys. (Paris) **39**, 951 (1978); L. Leibler, Macromolecules **15**, 1283 (1982).
[52] M. Takenaka, T. Hashimoto, and H. Jinnai (unpublished).
[53] T. Ohta and H. Nozaki, in *Space-Time Organization in Macromolecular Fluids,* edited by F. Tanaka, M. Doi, and T. Ohta (Springer-Verlag, New York, 1989).
[54] K. Kubota, N. Kuwahara, H. Eda, and M. Sakazume, Phys. Rev. A **45**, R3377 (1992).
[55] According to the prediction of Furukawa's equation [Eq. (12)] and with the parameters used above, the late stage of spinodal decomposition is estimated to be $\tau > \sim 100$ or $Q_m(\tau)M < \sim 0.1$ and is far beyond the present experimental time range.